ELSEVIER

Earth and Planetary Science Letters 140 (1996) 269–279

EPSL

Bubble size distribution in magma chambers and dynamics of basaltic eruptions

Sylvie Vergniolle *

Institute of Theoretical Geophysics, Department of Applied Maths and Theoretical Physics, 20 Silver Street, Cambridge CB3 9EW, United Kingdom

Received 12 July 1995; accepted 28 February 1996

Abstract

In the shallow magma chambers of volcanoes, the CO_2 content of most basaltic melts is above the solubility limit. This implies that the chamber contains gas bubbles, which rise through the magma and expand. Thus, the volume of the chamber, its gas volume fraction and the gas flux into the conduit change with time in a systematic manner as a function of the size and number of gas bubbles. Changes in gas flux and gas volume are calculated for a bubble size distribution and related to changes in eruption regimes. Fire fountain activity, only present during the first quarter of the eruption, requires that the bubbles are larger than a certain size, which depends on the gas flux and on the bubble content [1]. As the chamber degasses, it loses its largest gas bubbles and the gas flux decreases, eventually suppressing the fire fountaining activity. Ultimately, an eruption stops when the chamber contains only a few tiny bubbles. More generally, the evolution of basaltic eruptions is governed by a dimensionless number, $\tau^* = \tau g \Delta\rho a_o^2/(18\mu h_c)$, where τ = a characteristic time for degassing; a_0 = the initial bubble diameter; μ = the magma viscosity; and h_c = the thickness of the degassing layer. Two eruptions of the Kilauea volcano, Mauna Ulu (1969–1971) and Puu O'o (1983–present), provide data on erupted gas volume and the inflation rate of the edifice, which help constrain the spatial distribution of bubbles in the magma chamber: bubbles come mainly from the bottom of the reservoir, either by in situ nucleation long before the eruption or within a vesiculated liquid. Although the gas flux at the roof of the chamber takes similar values for both eruptions, the duration of both the fire fountaining activity and the entire eruption was 6 times shorter at Mauna Ulu than during the Puu O'o eruption. The dimensionless analysis explains the difference by a degassing layer 6 times thinner in the former than the latter, due to a 2 year delay in starting the Mauna Ulu eruption compared to the Puu O'o eruption.

Keywords: Kilauea; effusion; degassing; gaseous phase; carbon dioxide

1. Introduction

When basaltic melts are formed, they contain enough carbon dioxide to be above the solubility limit at depths of several kilometres [2–6], where most of magma reservoirs are located. The very existence of a gas phase makes models of basaltic volcanoes difficult, as the erupted lava represents only one component of the mixture issued from the reservoir. However, eruption parameters and conditions must evolve in a specific manner as degassing proceeds, which may shed light on the behaviour of the magma chamber. In particular, if gas is responsi-

* Present address: Laboratoire de Dynamique des Systémes Géologiques Institut de Physique du Globe 4 place Jussieu, 75252 Paris Cedex 05 France. E-mail: vergniolle@ipgp.jussieu.fr

PII S0012-821X(96)00042-8

ble for triggering eruption [7], one wishes to know the initial spatial distribution of bubbles before an eruption to infer their origin and initial depth of formation.

A consequence of gas in basaltic magma chambers is the formation of a gas-rich upper layer at its roof and, hence, the presence of two different reservoirs of gas: one made of isolated bubbles rising in the chamber interior and the other made of bubbles trapped at the roof and forming a foam. This leads to an intermittent behaviour during basaltic eruptions with alternating phases of gas-rich explosions, called fire fountains at Hawaii, and gas-poor lava effusion [1,8,9]. A fire fountain, a gas jet driving lava clots, is produced when the foam trapped at the roof becomes unstable and collapses [1,10]. The duration between two successive fire fountains, about 1 month, corresponds to the time to re-build the foam. After approximately one quarter of the duration of the eruption, the cyclic activity between fire fountains and lava effusion gives way to continuous lava effusion. This sharp change in eruption regime occurs when the gas flux decreases below a critical level [1]. However, the foam is still producing a few, smaller gas pockets [1,8,9], called 'gas pistons' at Hawaii [11,12], showing that some gas is still present in the volcanic system. Even if one can estimate the bubble size in the magma chamber when the fire fountain activity stops [1,13], it is still uncertain whether the end of this activity is due to a sharp change in the magma chamber or results from a continuous process.

When a magma containing gas bubbles is emplaced rapidly in a chamber of finite thickness [14], the bubbles rise, changing the vertical profile of the gas volume fraction and hence of the density in the chamber. Thus, the total volume of the chamber changes with time, and inflation occurs, which may be detected at the Earth's surface. At the Kilauea volcano (Hawaii), summit tilt deformations [11,12,15,16], appear to be clearly correlated with eruptive activity for both the Mauna Ulu (1969–

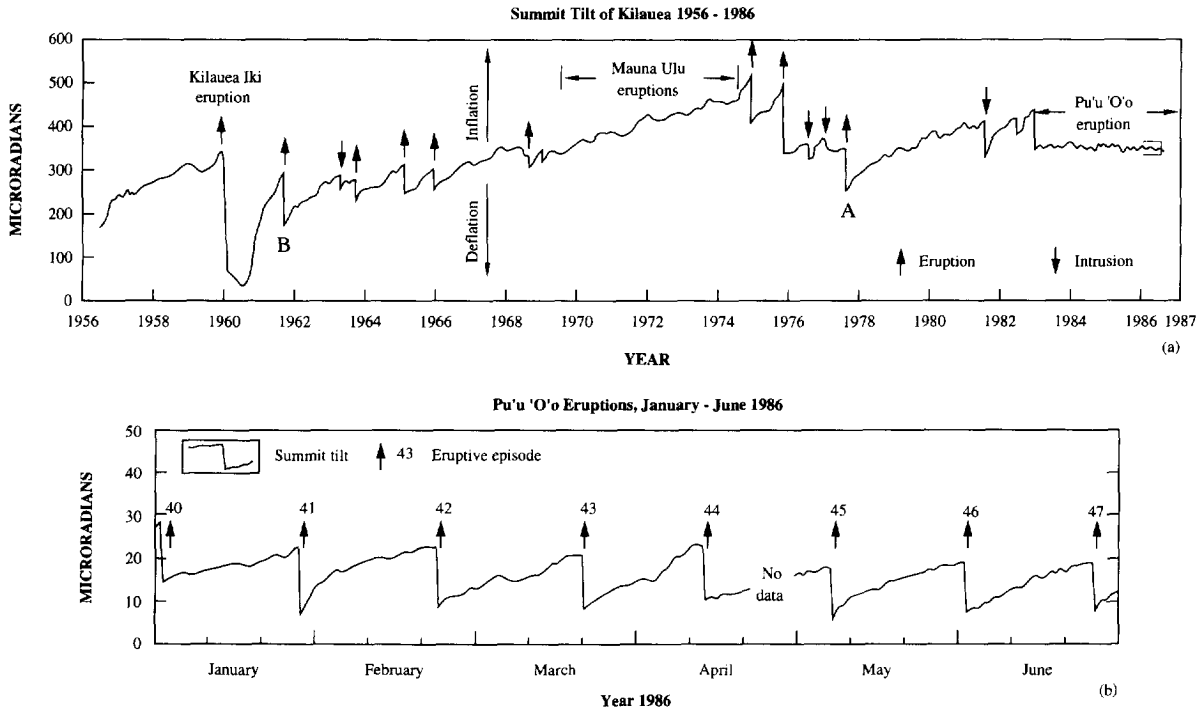

Fig. 1. Summit tilt deformation (East–West component) at Uwekahuna (Kilauea volcano, Hawaii). Above: since 1956. Points A and B are the onset of inflation at Puu O'o and Mauna Ulu (see text). Below: for the last episodes of fire fountains during the Puu O'o eruption (from [16]). The two eruptions of Mauna Ulu, 1969–1971 (studied in this paper) and 1972–1974, are shown by the same arrow.

1971) [11], and Puu O'o eruptions (1983–present) [12,16] (Fig. 1 above). Deformations are cyclic for the first quarter of the eruption, with slow inflation before each fire fountain and quick deflation at the end of each fire fountain (Fig. 1 below). Such deformations were previously explained only by liquid movement into and out of the magma chamber [11,17–19]; however, both the strong extension of the summit during the Puu O'o eruption [19] and the low level of seismicity before this eruption [17] suggests that gas is partly responsible for deformations, as also proposed by [20]. In addition, changes in gas volume are not negligible compared to changes in liquid volume [1]. It is therefore tempting to study how gas volume in the magma chamber changes with time.

It is possible, from a given bubble size distribution in the magma chamber, to calculate the evolution of gas volume and gas flux at the roof. These coupled quantities change with time, reflecting the evolution of the bubble population in the chamber. By comparing the model predictions to measurements of volume and flux during Puu O'o and Mauna Ulu eruptions of Kilauea volcano, it is hoped to constrain the temporal and spatial bubble distribution in the chamber, which is still poorly known. This can then be used to understand factors which control the duration of both the cyclic activity and the eruption.

2. Physical framework

Due to the fact that the solubility of CO_2 (0.0543 wt% for a pure CO_2 phase at 1 kbar and 1200°C [4]) is much less than the total CO_2 concentration (0.32 wt% [21]) the magma is saturated everywhere in the chamber, at least in CO_2. Therefore, one can consider the magma chamber as a reservoir containing a liquid phase and an initial population of gas bubbles (Fig. 2a). The part which contains exsolved bubbles is called the degassing layer. The gas bubbles rise and expand in response to the external pressure gradient, here assumed to be lithostatic. Bubbles are assumed to be in chemical equilibrium with their surroundings, because the diffusion of chemical species into the bubble, controlled by the local concentration of volatile species, cannot be easily assessed. Hence, the bubble growth is mainly a consequence of decompression due to rise, giving a lower bound to both the bubble size and gas flux. The gas is also assumed to behave ideally, which is valid at depths of a few kilometres [14]. The gas volume fraction in the magma chamber is small [1], and hence each bubble may be treated as isolated. Therefore, the evolution during time of the bubble diameter depends only on the initial depth of each bubble and its velocity.

2.1. Equations for a single bubble

Because bubbles are small, less than 1 mm [1], and rise slowly, they are in permanent equilibrium with the surrounding magma. Hence, assuming an isothermal ascent path, the bubble diameter, a, at depth z depends on initial bubble size, a_o, and initial depth, z_o (Fig. 2a):

$$a = a_o \left(\frac{z_c + h_c - z_o}{z_c + h_c - z} \right)^{1/3} \tag{1}$$

where z_c and $(z_c + h_c)$ are the depths of the top and bottom of the chamber, respectively. For a magma viscosity $\mu = 10$ Pa · s, bubbles smaller than 5 cm, as in magma chamber [1], can be considered as small and rise with their Stokes velocity [22]. In addition, because their surface is probably covered by tiny crystals, bubbles can be considered as rigid spheres and their velocity, $V(t)$, is [22]:

$$V(t) = \frac{\mathrm{d}z}{\mathrm{d}t} = \frac{a^2 g \Delta\rho}{18\mu} \tag{2}$$

where $\Delta\rho$ is the density difference between liquid and gas. As a bubble rises, its size increases and the volume of displaced liquid around it increases. However, for small velocities (1.5×10^{-4} m/s for a bubble diameter of 1 mm), the acceleration of the 'added' mass can be neglected [22]. Using Eqs. (1) and (2), time t and bubble diameter a are related to each other through the following equations:

$$t(z) = \left[1 - \left(\frac{z_c + h_c - z}{z_c + h_c - z_o} \right)^{5/3} \right] (z_c + h_c - z_o) \times \frac{3 \times 18\mu}{5\Delta\rho g a_o^2} \tag{3}$$

$$a = a_o \left(1 - \frac{5 t a_o^2 g \Delta\rho}{3 \times 18\mu (z_c + h_c - z_o)} \right)^{-1/5} \tag{4}$$

The maximum increase in the gas volume is obtained for a bubble starting to rise at the bottom of the magma chamber. It is limited to a factor of 2 in a chamber 2 km deep and 2 km high, as at Kilauea, and is faster for a large bubble than for a smaller one.

Because it controls the rate and amount of gas emitted at the surface, which can be measured, the gas flux at the roof of the magma chamber is an essential quantity to be determined. If it is straightforward to calculate when and how much gas reaches the top of the magma chamber for a single bubble, this becomes more difficult when bubbles of different sizes and initial depths are present in the reservoir. At a given time, t, the gas flux at the roof will result from small bubbles that started not far below the top of the magma chamber and from large bubbles that originated at greater depths (Fig. 2b). For instance, with initial bubble diameters between 0.1 and 1 mm, as for Kilauea [1], it takes a month to

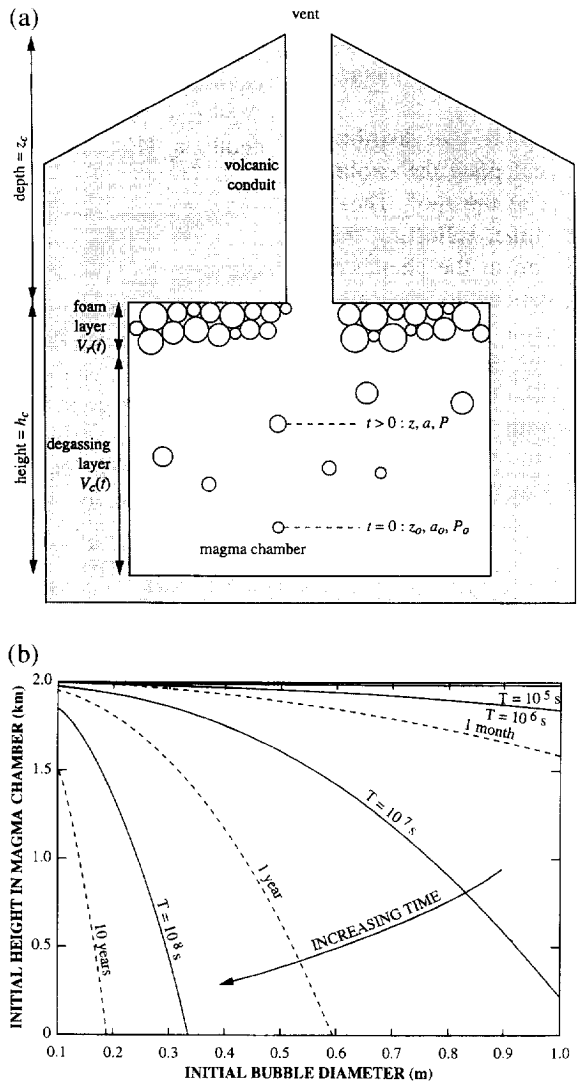

Fig. 2. (a) Sketch of a degassing magma chamber. (b) Time, from 1 month to 10 yr, to reach the roof for different initial bubbles starting from different depths.

collect bubbles of all sizes from the uppermost 400 m. After 4 months, the largest bubbles (1 mm) that started at the bottom of the chamber have reached the roof. After 1 yr only bubbles with an initial diameter less than 0.6 mm still arrive at the top. It is therefore clear that the gas flux at the roof will depend strongly on the size and number of bubbles and that the duration of an eruption will depend on the bubble size and the height of the magma chamber.

2.2. Gas flux and gas volume for a bubble distribution

At some initial time, the mixture of stagnant magma and bubbles, with a given size distribution, is left to evolve by itself, without generation of new bubbles, for several years, the typical duration of a Hawaiian eruption. Because there is a unique combination of initial diameter a_o and depth z_o which gives a bubble diameter a at depth z and time t, the number per meter height $N(t,z,a)$ of bubbles having diameter a at time t and at depth z is:

$$N(t,z,a) = N(0,z_o,a_o) \tag{5}$$

where a is given by Eq. (4). The gas volume $\mathrm{d}V(t,z)$ between depths z and $z+\mathrm{d}z$, and the gas flux $Q(t,z)$ at depth z are given by:

$$\mathrm{d}V(t,z) = \left[\int_{a=0}^{+\infty} N(t,z,a)\,\frac{\pi a^3}{6}\,\mathrm{d}a\right]\mathrm{d}z \tag{6}$$

$$Q(t,z) = \int_{a=0}^{+\infty} N(t,z,a)\,\frac{\pi a^3}{6}\,\frac{a^2 g\,\Delta\rho}{18\mu}\,\mathrm{d}a \tag{7}$$

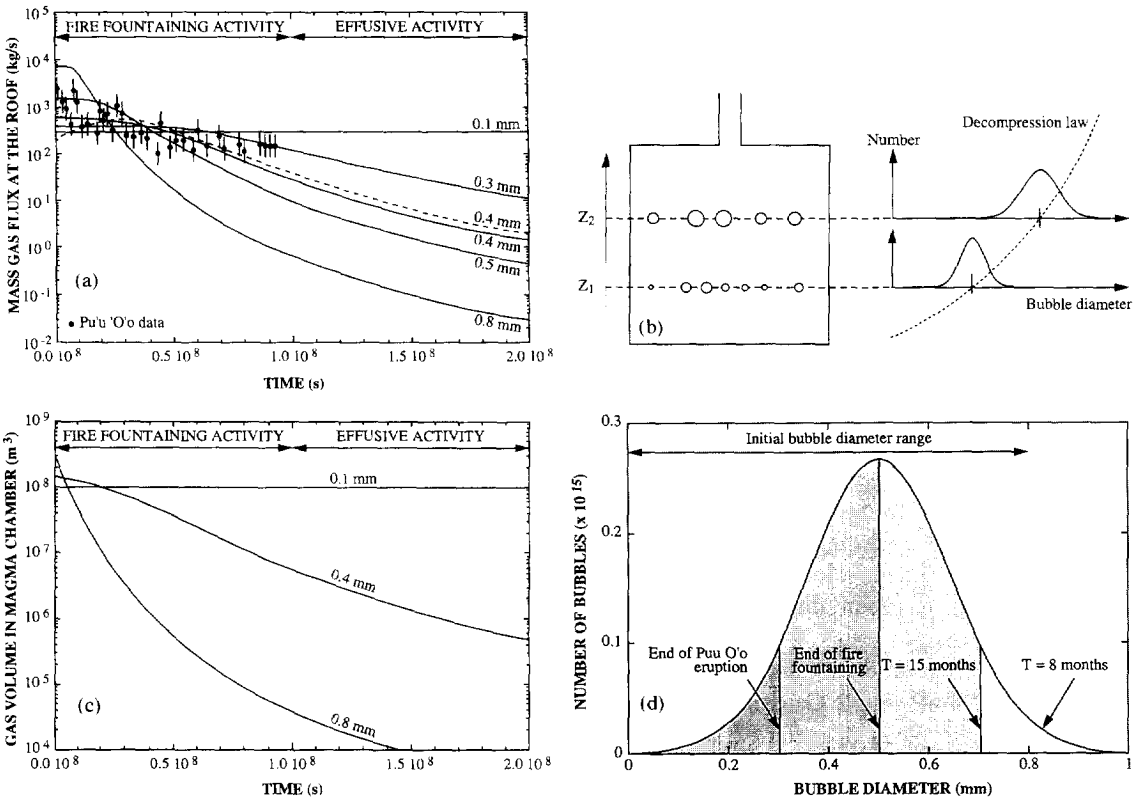

Fig. 3. (a) Measurements of mass gas flux at the roof during fire fountains of the Puu O'o eruption, 1983–1986. Dashed line is calculated flux assuming an uniform initial diameter a_o of 0.4 mm throughout the chamber. Errors bars reflect uncertainties in gas velocity (see text). Solid lines are calculated flux assuming initial diameters of a_o of 0.1, 0.3, 0.4, 0.5 and 0.8 mm, reflecting vertical pressure gradient. (b) Sketch of a magma chamber in which initial average bubble diameter, a_o, reflects decompression. (c) Calculated gas volume in the degassing layer for a_o = 0.1, 0.4 and 0.8 mm. (d) Bubble size distribution at top of degassing layer for 4 different values (8, 15, 42 months and 6 yr) of time elapsed since the beginning of the Puu O'o eruption.

At time t, the volume of gas trapped in the foam at the roof (Fig. 2a) is therefore:

$$V_r(t) = \int_{\tau=0}^{\tau=t} Q(\tau, h_c)\mathrm{d}\tau \quad (8)$$

Then, the volume of gas due to rising bubbles, $V_c(t)$ is:

$$V_c(t) = \int_{z=0}^{z=h_c} \mathrm{d}V(t,z) - V_r(t) \quad (9)$$

when ignoring gas leak and bubble exsolution.

Little is known about the distribution of bubbles diameters in a magma chamber. At the surface, lava flows, with gas volume fraction as high as 30%, exhibit complex size distribution, probably resulting from the coalescence of closely spaced bubbles [23–25]. At depths typical of magma chambers, the gas volume fraction is less than a few percent, preventing bubble coalescence. The bubble size distribution in the magma chamber should be comparable to the Gaussian distribution observed in basalts of mid-oceanic ridges [26], which are emplaced at similar depths, albeit at lower pressures; therefore, the bubble size distribution will be assumed to be Gaussian in the magma chamber. The average number of bubbles, N_i, per unit height, is assumed uniform throughout the chamber and the number of bubbles $N(0, z_o, a)$ is:

$$N(0, z_o, a) = \frac{N_i}{\sigma_o\sqrt{2\pi}} \exp\left[-\frac{(a-\bar{a})^2}{2\sigma_o^2}\right] \quad (10)$$

where $\bar{a}$ is the mean bubble diameter and σ_o is the standard deviation. A Gaussian distribution extends to infinity with negative values but, in practice, a distribution truncated outside the range $[\bar{a} - 3.5\sigma_o, \bar{a} + 3.5\sigma_o]$ is always used. σ_o is taken equal to $\bar{a}/3.5$, so that the minimum value of the distribution is close to 0 and the maximum diameter is twice the mean.

Two cases of Gaussian distribution can be envisaged. The first and most simple Gaussian distribution is one for which the mean diameter, $\bar{a}$, is uniform throughout the chamber. Such a distribution produces a mass fraction of gas increasing with depth. Shortly after the beginning of eruption, the bubbles which arrive at the roof have had little time to grow. Then, progressively larger bubbles reach the top because they have grown for longer times. Because bubbles which arrive at the roof of the magma chamber come from progressively deeper layers, which are richer in gas, the gas flux at the roof increases steadily at the beginning of the eruption, during 1 yr for a bubble diameter of 0.4 mm (Fig. 3a). After the last bubbles coming from the bottom of the magma chamber have arrived at the roof, the gas flux decreases because smaller and smaller bubbles, which make the left tail of the Gaussian distribution, arrive at the top. This increase, followed by a decrease in gas flux, does not depend on the average bubble diameter $\bar{a}$. Because such an initial increase in gas flux is not observed (Fig. 3a), a uniform Gaussian distribution with depth is, therefore, unlikely.

It is more realistic to envisage that the average diameter is depth-dependent, reflecting the vertical pressure gradient and corresponding to a uniform mass fraction of gas (Fig. 3b). This distribution either simulates a re-injection of vesiculated liquid in the magma chamber or is the result of the slow evolution of an existing bubble population, initially formed at the same depth, probably at the bottom of the magma chamber long before the eruption. The mean value, $\bar{a}(z)$, and the standard deviation, $\sigma_o(z)$, vary with depth as:

$$\bar{a}(z) = \bar{a}(z=0)\left(\frac{z_c + h_c - z}{z_c + h_c - z_o}\right)^{1/3} \quad (11)$$

$$\sigma_o(z) = \sigma_o(z=0)\left(\frac{z_c + h_c - z}{z_c + h_c - z_o}\right)^{1/3} \quad (12)$$

Since the initial distribution already reflects the increase in diameter with the rise of the bubbles, the number and sizes of bubbles which reach the top of the chamber and, therefore, the corresponding gas flux, remain constant. While the gas flux can remain constant for some time, the volume of gas due to rising bubbles decreases as soon as the eruption starts (Fig. 3c). This holds as long as the largest bubbles which start from the bottom have not reached the roof. When this happens, the bubble size distribution at the roof becomes truncated (Fig. 3d) and the gas flux at the roof begins to decrease (Fig. 3a). Because large bubbles rise faster, this change, from constant to decreasing gas flux, will occur sooner for larger values of initial bubble diameter, a_o (typically a few months after the beginning of eruption if it is

larger than 0.8 mm), than for smaller ones (a few years if the bubble diameter is equal to 0.4 mm). Therefore, the value of the initial diameter influences the shape of the evolution of the gas flux with time, while the initial number of bubbles per meter height, N_i, merely controls the actual value of this flux.

It has so far been assumed that the liquid is stagnant in the magma chamber. If there are strong convective motions in the chamber interior, it contains less and less bubbles with time as they escape towards the upper boundary layer close to the roof [27] with a velocity similar to those of the present model. Existing measurements, however, are not sufficient to suggest which model is the most appropriate.

3. Applications to Kilauea volcano, Hawaii

3.1. The Puu O'o eruption

As stated above, the only data which can constrain the model are the gas flux and gas volume measured at the surface. Although the gas flux at the roof of the magma chamber can vary with time, it behaves essentially in a continuous manner, whereas the gas flux at the surface is more discontinuous, with sudden bursts during fire fountains separated by quiet intervals. This behaviour has been explained by the regular emission of large gas pockets formed by the coalescence of the foam layer at the roof of the magma chamber [1,8,9]. If one assumes that the entire foam layer collapses during a fire fountain episode [8], the mass of gas emitted during such an episode must be equal to the mass of gas trapped in the foam layer, which is, in turn, equal to the mass flux of gas at the roof multiplied by the time interval between two successive fountain episodes [1].

The gas volume flux at volcanic vents is estimated from measurements of ejecta velocities [28], usually assumed to be equal to the gas velocity. If the motion of ejecta is purely inertial, the velocity at the vent v is related to the height of fire fountains, h, by $v = \sqrt{2gh}$ [28]. Taking air friction into account, for ejecta as large as 20 cm, as observed in 1983 [29], this velocity must be multiplied by a factor of 3 [30]. This uncertainty could be enlarged further by a factor of 2, because of the possible exsolution of water vapour in the conduit above the magma chamber [1]. The reservoir, with a thickness $h_c \approx 2$ km is located at a depth $z_c \approx 2$ km, as inferred from seismic studies [15,17,20,31,32]. Its area is at least 10 km^2 [1], giving a minimum volume of 2×10^{10} m^3.

During the cyclic activity of the Puu O'o eruption, the mass gas flux decreases from 5×10^3 to 3×10^2 kg/s, or from 1.7×10^3 to 10^2 kg/s, depending on the determination of gas velocity. This slow decrease is best reproduced if the initial bubble diameter at the bottom of the chamber is 0.4 mm (Fig. 3a), corresponding to the theoretical diameter for a bubble growing by decompression and diffusion at a depth of 4 km [14,33]. Allowing for possible changes in ejecta size over that period of time brings an uncertainty of 0.1 mm around the central value of 0.4 mm (Fig. 3a). With these values, the average number of bubbles per meter height in the chamber is $N_i = 7.5 \times 10^{14}$, giving initial gas volume fractions of 0.05% and 0.5% at the bottom and the top of the magma chamber, respectively. These values are comparable to the lowest estimates of gas volume fraction in mid-oceanic ridges basalts [26], which are emplaced at similar depths but lower pressures. Plotting the evolution of the bubble size distribution at the roof (Fig. 3d) shows that the end of fire fountaining activity occurs when bubbles with diameter above the mean value of 0.5 mm at the roof have all disappeared from the degassing layer. Because bubbles remaining in the chamber are few and small, and therefore rise slowly, the gas flux is now too low to drive further fountain activity. It is still capable, however, of generating gas piston activity for several years, superimposed on quiet effusive activity [11,12]. The calculated gas volume in the degassing layer decreases strongly until it represents less than 1% of its initial value at the end of the eruption (Fig. 3c,d).

3.2. Mauna Ulu eruption

The Mauna Ulu eruption shares several features with the Puu O'o eruption [11,12,16]. The values of gas flux at the roof at the beginning of the eruption, 10^4 kg/s, and at the end of fire fountain activity,

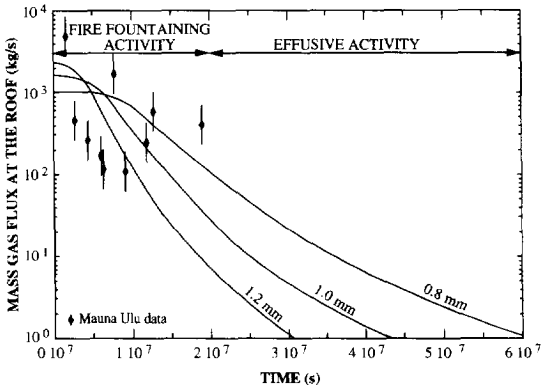

Fig. 4. Measurements of mass gas flux at the roof during fire fountains of the Mauna Ulu eruption, 1969–1971. Error bars as in Fig. 3a. Solid lines are calculated gas flux for height $h_c = 2$ km and $a_o = 0.8$, 1 and 1.2 mm. Results for $h_c = 330$ m, $a_o = 0.4$ mm and $h_c = 500$ m, $a_o = 0.5$ mm are undistinguishable from $a_o = 1$ mm and $h_c = 2$ km.

2×10^2 kg/s, are of similar orders. The time interval between two successive fire fountains is also similar, about 1 month. The major difference between both eruptions is that the Mauna Ulu eruption was approximately 6 times shorter than the Puu O'o eruption, both in terms of duration of fire fountain activity (7 months versus 42 months) and the total length of the eruption. If the average initial bubble diameter at the bottom of the degassing layer were also 0.4 mm, the Mauna Ulu eruption would result from the degassing of a much thinner layer, 330 m instead of 2 km for the Puu O'o eruption and with a number of bubbles per meter height, N_i, equal to 5×10^{15} (Fig. 4). Because both eruptions were located not far from each other in the East Rift zone [12], it is probable that they have been fed by the same magma chamber, 2 km high at a depth of 2 km. In that case, accounting for uncertainties in gas flux measurements, the average initial bubble diameter at Mauna Ulu is 1 ± 0.2 mm (Fig. 4), 2.5 times larger than at Puu O'o and the number of bubbles per meter height is 1.5×10^{13}. Unless independent constraints are brought in, for example from studies on the nucleation and growth of bubbles [33–35], it is difficult at this stage to decide whether the degassing layer was 330 m with a bubble diameter of 0.4 mm, or 2 km with a diameter of 1 mm, before the Mauna Ulu eruption.

3.3. Characteristic time

The trade-off between the bubble diameter and the height of the magma chamber can be easily understood. Neglecting its increase in volume, a bubble of initial diameter a_o takes on average time t_c:

$$t_c = \frac{h_c}{V(t)} = \frac{18 \mu h_c}{a_o^2 g \Delta \rho} \tag{13}$$

to rise from the bottom to the top of the chamber, h_c. If τ_f is the duration of fire fountain activity, it has a non-dimensional equivalent τ_f^*:

$$\tau_f^* = \frac{\tau_f}{t_c} = \tau_f \frac{a_o^2 g \Delta \rho}{18 \mu h_c} \tag{14}$$

From values of the initial diameter, a_o, and height of the degassing layer, h_c, which fit best the gas flux, τ_f^* has values of 1.1 and 1.3 for Puu O'o and Mauna Ulu eruptions, respectively. Similarly, if one scales the total duration of the eruption τ_e by the same factor t_c, one has τ_e^* equal to 4.2 and 4.3 for Puu O'o and Mauna Ulu eruptions, respectively. The fact that τ_e^* is about four times τ_f^* suggests that an eruption stops when bubbles with an initial diameter of half the average diameter a_o have reached the roof. This near coincidence in both τ_f^* and τ_e^* suggests that basaltic eruptions are fundamentally controlled by the same physical process: the complete degassing of the magma chamber, regardless of its dimensions and of the size of bubbles.

4. Discussion

The natural diameter of bubbles at a depth of 4 km is around 0.4 mm [14,33], an initial diameter of 1.0 mm at the same depth could be explained, for instance, by coalescence. This would reduce the number of bubbles by a factor of $(1/0.4)^3 \approx 16$. Accounting for uncertainties in gas flux measurements, this could explain part of the approximately 50 times decrease in the total bubble number between the Puu O'o and Mauna Ulu eruptions. However, given the low gas volume fraction (at most 1%) coalescence is unlikely [22].

It has been shown that taking bubbles with an

initial diameter between 0.4 and 0.5 mm at Mauna Ulu provides a total number of bubbles similar to that calculated at Puu O'o but implies a much thinner degassing layer: 300–500 m, instead of 2000 m. This can be explained by the following scenario: Although the initial bubble population at Mauna Ulu was similar in size and number to that of Puu O'o, it stayed a longer time in the chamber before the eruption started. Therefore, the bubbles had time to grow slightly and rise in the chamber. From Eq. (2), a 0.4 mm large bubble takes about 2 yr to rise from a depth of 4 km to a depth of 2.5–2.8 km. One can note that Puu O'o eruption started in 1983, 6 years after an eruption in 1977 (point A, Fig. 1a), marked by a sudden and strong deflation (≈ 100 μrd) of the Kilauea summit, and that the Mauna Ulu eruption started about 8 years after an eruption in 1961 (point B, Fig. 1a), also marked by a sudden and equally strong deflation. In addition, the total number of bubbles in the chamber prior to eruption was $N_i \times h_c = 1.5 \times 10^{18}$ at Puu O'o and $N_i \times h_c = 1.65 \times 10^{18}$ at Mauna Ulu. Although it may be a pure coincidence, this has the merit of explaining both eruptions within a single framework with one slight difference, which is supported by observations.

A fundamental hypothesis of the model proposed here is that there is no addition of gas in the chamber as the eruption proceeds. The net volume change between the beginning and the end of the eruption should thus be negative. Summit deformations show, however, that there is almost no volume change during the Puu O'o eruption and that the Mauna Ulu eruption is superimposed on a general inflation (Fig. 1a), suggesting that there is indeed re-injection of magma or formation of tiny bubbles at depth.

Measurements of volumes of gas, calculated at the pressure of the chamber, and of liquid expelled during each fire fountain at Puu O'o [1], show that a total of $56 \pm 11 \times 10^7$ m^3 were expelled during most of the fire fountain phase. Therefore, $16 \pm 3 \times 10^7$ m^3 should be injected per year to balance the loss at the surface during the 3.5 year long Puu O'o fire fountain activity. This is slightly above, but comparable to, the magma supply rate of 13×10^7 m^3/yr calculated by [12].

From volumes of liquid and gas expelled during fire fountains of the Mauna Ulu eruption and associated tilt variations [11], there is a deflation of 1.4 ± 0.6 μrd per 10^6 m^3 of expelled volume. Taking this rate to hold during the general inflation observed during the Mauna Ulu eruptions, the ≈ 20 μrd cumulated during the 7 months of long cyclic activity results from a net increase of $1.4 \pm 0.6 \times 10^7$ m^3. Given a total expelled volume of $12.4 \pm 3.2 \times 10^7$ m^3, over that period [11], the volume injected at depth should be $13.8 \pm 3.8 \times 10^7$ m^3, giving a yearly average of $24 \pm 7 \times 10^7$ m^3. This is a little higher than what was obtained for the Puu O'o eruption, but probably not significantly, given the various uncertainties discussed above. In both cases, the volume re-injected per year represents only 1% of the estimated volume of the magma, $\approx 2 \times 10^{10}$ m^3 in the chamber.

The exact partitioning between gas and liquid in the $\approx 2 \times 10^8$ m^3/yr influx rate at depth cannot be easily constrained. The proportion of gas must not be too high, however, otherwise the cyclic activity would never stop. The critical gas flux, calculated at a depth of 4 km, necessary to feed fire fountains at the top is $\approx 1.5 \times 10^7$ m^3/yr [1]. Therefore, the volume fraction of gas does not exceed 7.5% of the $\approx 2 \times 10^8$ m^3/yr re-injected at depth. In fact, it is probably much lower than that. Typical gas volume fractions at 4 km are at most 1% [36]. The gas influx rate at depth is therefore of the order of 10^6 m^3/yr. Since it is not enough to trigger and maintain fire fountains, it is necessary to call for another mechanism capable of generating enough bubbles: for instance, long-term cooling and crystallisation in the magma chamber can produce gas in amounts large enough to trigger eruptions [7].

5. Conclusion

The evolution, in a closed reservoir, of a Gaussian population of bubbles, with the average diameter decreasing with depth, provides a simple explanation for the dynamics of Hawaiian basaltic eruptions. The cyclic activity lasts until the largest bubbles have risen from the bottom of the magma chamber. At that time, the gas flux, which has decreased continuously since the onset of eruption, becomes too low to feed fire fountains. After that, a quiet effusive activity with gas piston events takes place, until about 1% of the initial gas volume remains in the chamber.

From measurements of gas flux during the Puu O'o and Mauna Ulu eruptions, the initial diameter of bubbles was 0.4 ± 0.1 mm, in a 2 km thick layer for Puu O'o and in a 300–500 m thick layer for Mauna Ulu. This difference can be explained by the fact that bubbles had 8 years to evolve prior to the Mauna Ulu eruption instead of 6 years for Puu O'o eruption. At Puu O'o, the gas volume fraction is between 0.05% and 0.5%. From summit tilt deformations and volumes of gas and liquid expelled during fire fountains, an estimate of 2×10^8 m^3 of magma is re-injected each year into the magma chamber.

Acknowledgements

This paper has greatly benefitted from useful discussions with C. Jaupart and critical reviews by R.S.J. Sparks, Y. Bottinga, R.C. Kerr and Y. Gaudemer. The work was supported by a EEC grant number SC1* CT005010. *[PT]*

References

[1] S. Vergniolle and C. Jaupart, Dynamics of degassing at Kilauea volcano, Hawaii, J. Geophys. Res. 95, 2793–2809, 1990.

[2] T.M. Gerlach and E. Graeber, Volatile budget of Kilauea volcano, Nature 313, 273–277, 1985.

[3] E. Stolper and J.R. Holloway, Experimental determination of the solubility of carbon dioxide in molten basalt at low pressure, Earth Planet. Sci. Lett. 87, 397–408, 1988.

[4] V. Pan, J.R. Holloway and R.L. Hervig, The pressure and temperature dependence of carbon dioxide solubility in tholeiitic basalt melts, Geochim. Cosmochim. Acta 55, 1587–1595, 1991.

[5] A.R. Pawley, J.R. Holloway and P.F. McMillan, The effect of oxygen fugacity on the solubility of carbon–oxygen fluids in basaltic melt, Earth Planet. Sci. Lett. 110, 213–225, 1992.

[6] T.M. Gerlach and B.E. Taylor, Carbon isotope constraints on degassing of carbon dioxide from Kilauea volcano, Geochim. Cosmochim. Acta 54, 2051–2058, 1990.

[7] S.R. Tait, C. Jaupart and S. Vergniolle, Pressure, gas content and eruption periodicity of a shallow crystallising magma chamber, Earth Planet. Sci. Lett. 92, 107–123, 1989.

[8] C. Jaupart and S. Vergniolle, The generation and collapse of a foam layer at the roof of a basaltic magma chamber, J. Fluid. Mech. 203, 347–380, 1989.

[9] C. Jaupart and S. Vergniolle, Laboratory models of Hawaiian and Strombolian eruptions, Nature 331, 58–60, 1988.

[10] S. Vergniolle and C. Jaupart, Separated two-phase flow and basaltic eruptions, J. Geophys. Res. 91, 12842–12860, 1986.

[11] D.A. Swanson, D.A. Duffield, D.B. Jackson and D.W. Peterson, Chronological narrative of the 1969–1971 Mauna Ulu eruption of Kilauea volcano, Hawaii, U.S. Geol. Surv. Prof. Pap. 1056, 1–55, 1979.

[12] E.W. Wolfe, M.O. Garcia, D.B. Jackson, R.Y. Koyanagi, C.A. Neal and A.T. Okamura, The Puu O'o eruption of Kilauea volcano, episodes 1–20, January 3, 1983 to June 8, 1984, U.S. Geol. Surv. Prof. Pap. 1350, 471–508, 1987.

[13] S. Vergniolle and C. Jaupart, Degassing processes in a magma chamber during an eruption (Hawaian case), IUGG XX Assembly, IAVCEI Program and abstracts 33, 1991.

[14] Y. Bottinga and M. Javoy, Mid-oceanic ridge basalt degassing: bubble nucleation, J. Geophys Res. 95, 5125–5131, 1990.

[15] J.J. Dvorak and A.T. Okamura, Variations in tilt rate and harmonic tremor amplitude during the January–August 1983 East-Rift eruptions of Kilauea volcano, Hawaii, J. Volcanol. Geotherm. Res. 25, 249–258, 1985.

[16] R.I. Tilling, C. Heliker and T.L. Wright, Eruptions of Hawaiian volcanoes: past, present, future, Dept. Interior/U.S. Geological Survey, 1987.

[17] F.W. Klein, R.Y. Koyanagi, J.S. Nakata and W.R. Tanigawa, The seismicity of Kilauea's magma system, U.S. Geol. Surv. Prof. Pap. 1350, 1019–1186, 1987.

[18] E.A. Parfitt and L. Wilson, The 1983–1986 Puu O'o eruption of Kilauea volcano, Hawaii: a study of dike geometry and eruption mechanisms for a long-lived eruption, J. Volcanol. Geotherm. Res. 59, 179–205, 1994.

[19] P.T. Delaney, A. Miklius, T. Arnadottir, A.T. Okamura and M.K. Sato, Motion of Kilauea volcano during eruption from the Puu O'o and Kupaianaha vents, 1983–1991, J. Geophys. Res. 98, 17801–17820, 1993.

[20] D.J. Johnson, Dynamics of magma storage in the summit reservoir of Kilauea volcano, Hawaii, J. Geophys. Res. 97, 1807–1820, 1992.

[21] L.P. Greenland, Gases from the 1983–1984 east-rift zone eruption, The Puu O'o eruption of Kilauea Volcano, Hawaii: episodes 1 through 20, January 3 1983 through June 8, 1984, U.S. Geol. Surv. Prof. Pap. 1463, 145–153, 1989.

[22] R. Clift, J.R. Grace and M.E. Weber, Bubbles, Drops and Particles, 380 pp., Academic Press, London, 1978.

[23] K.V. Cashman, M.T. Mangan and S. Newman, Surface degassing and modifications to vesicle size distributions in active basalt flows, J. Volcanol. Geotherm. Res. 61, 45–68, 1994.

[24] G.P.L. Walker, Spongy pahoehoe in Hawaii: a study of vesicle-distribution patterns in basalt and their significance, Bull. Volcanol. 51, 199–209, 1989.

[25] D.L. Sahagian, A.T. Anderson and B. Ward, Bubble coalescence in basalt flows: comparison of a numerical model with natural examples, Bull. Volcanol. 52, 49–56, 1989.

[26] P. Sarda and D. Graham, Mid-ocean ridge popping rocks: implications for degassing at ridge crests, Earth Planet. Sci. Lett. 97, 268–289, 1990.

[27] D. Martin and R. Nokes, Crystal settling in a vigorously convective magma chamber, Nature 332, 534–536, 1988.

[28] L. Wilson, Relationship between pressure, volatile content

and ejecta velocity in three types of volcanic eruptions, J. Volcanol. Geotherm. Res. 8, 297–313, 1980.

[29] T.J. Takahashi and J.D. Griggs, Hawaiian volcanic features: A photoglossary, U.S. Geol. Surv. Prof. Pap. 1350, 845–902, 1987.

[30] M. Bursik, Effects of the drag force on the rise height of particles in the gas-thrust region of volcanic eruption columns, Geophys. Res. Lett. 16, 5, 441–444, 1989.

[31] R.Y. Koyanagi, J.T. Unger, E.T. Endo and A.T. Okamura, Shallow earthquakes associated with inflation episodes at the summit of Kilauea volcano, Hawaii, Bull. Volcanol. 39, 621–631, 1976.

[32] M.P. Ryan, The mechanics and three-dimensional internal structure of active magma systems: Kilauea volcano, Hawaii, J. Geophys. Res. 93, 4213–4248, 1988.

[33] Y. Bottinga and M. Javoy, The degassing of Hawaiian tholeiite, Bull. Volcanol., 53, 73–85, 1991.

[34] A. Toramaru, Numerical study of nucleation and growth of bubbles in viscous magmas, J. Geophys. Res. 100, 1913–1931, 1995.

[35] R.S.J. Sparks, The dynamics of bubble formation and growth in magmas: a review and analysis, J. Volcanol. Geotherm. Res. 3, 1–37, 1978.

[36] J.G. Moore, Petrology of deep-sea basalt near Hawaii, Am. J. Sci. 263, 40–52, 1965.